Cellular Signalling 28 (2016) 1593–1603

Contents lists available at ScienceDirect

Cellular Signalling

journal homepage: www.elsevier.com/locate/cellsig

DNA Topoisomerase IIα contributes to the early steps of adipogenesis in 3T3-L1 cells

Rhîan G. Jacobsen [a], Fatemeh Mazloumi Gavgani [a], Gunnar Mellgren [b], Aurélia E. Lewis [a,*]

[a] NucReg Research Program, Department of Molecular biology, University of Bergen, Norway
[b] Hormone Laboratory, Haukeland University Hospital, KG Jebsen Center for Diabetes Research, Department of Clinical Science, University of Bergen, Bergen, Norway

ARTICLE INFO

Article history:
Received 20 May 2016
Accepted 7 July 2016
Available online 9 July 2016

Keywords:
DNA Topoisomerase II
Class I PI3K
Adipogenesis
PPARγ

ABSTRACT

DNA topoisomerases (Topo) are multifunctional enzymes resolving DNA topological problems such as those arising during DNA replication, transcription and mitosis. Mammalian cells express 2 class II isoforms, Topoisomerases IIα (Topo IIα) and IIβ (Topo IIβ), which have similar enzymatic properties but are differently expressed, in dividing and pluripotent cells, and in post-mitotic and differentiated cells respectively. Pre-adipocytes re-enter the cell cycle prior to committing to their differentiation and we hypothesised that Topo II could contribute to these processes. We show that Topo IIα expression in 3T3-L1 cells is induced within 16 h after the initiation of the differentiation programme, peaks at 24 h and rapidly declines thereafter. In contrast Topo IIβ was present both in pre-adipocytes and throughout differentiation. Inhibition of PI3K with LY294002, known to prevent adipocyte differentiation, consistently reduced the expression of Topo IIα, whereas a clear effect on Topo IIβ was not apparent. In addition, inhibition of mTOR with rapamycin also reduced the protein levels of Topo IIα. Using specific class IA PI3K catalytic subunit inhibitors, we show that p110α inhibition with A66 has the greatest reduction of Topo IIα expression and of differentiation, as measured by triglyceride storage. The timing of Topo IIα expression coincides with the mitotic clonal expansion (MCE) phase of differentiation and inhibition of Topo II with ICRF-187 during this stage decreased PPARγ1 and 2 protein levels and triglyceride storage, whereas inhibition later on has little impact. Moreover, the addition of ICRF-187 had no effect on the incorporation of EdU during S-phase at day 1 but lowered the relative cell numbers on day 2. ICRF-187 also induced an increase in the centri/pericentromeric heterochromatin localisation of Topo IIα, indicating a role for Topo IIα at these locations during MCE. In summary, we present evidence that Topo IIα plays an important role in adipogenesis during MCE and in a PI3K/mTOR-dependent manner. Considering that Topoisomerases II are targets in cancer chemotherapy, our results highlight that treatment of cancer with Topo II inhibitors may alter metabolic processes in the adipose tissue.

1. Introduction

Obesity, a disorder characterised by an increase in white adipose tissue mass, is a major risk for the development of type II diabetes, cardiovascular diseases, and some cancers [1]. Increased white adipose tissue mass is believed to be due to, not only adipocyte hypertrophy, but also hyperplasia [2]. Although extensively studied, the molecular mechanisms regulating these processes are however not fully understood and warrant further research efforts.

The 3T3-L1 pre-adipocyte cell line has provided much of our knowledge in the adipocyte differentiation processes [3]. Following cell cycle arrest, these cells respond to the combined treatment of differentiation inducers, consisting of 3-isobutyl-1-methylxanthine (IBMX), dexamethasone and insulin, re-enter the cell cycle for about 2 rounds of mitosis, before the induction of terminal differentiation [4]. Cell cycle re-entry, a process also called mitotic clonal expansion (MCE), followed by cell cycle arrest, is thought to be required for terminal differentiation of adipocytes [4,5]. DNA replication is thought to permit the re-organisation of the chromatin landscape necessary for the initiation of adipogenic gene expression orchestrated by the nuclear receptors CCAAT/enhancer-binding protein (C/EBP) β and peroxisome proliferator-activated receptor γ (PPARγ) [6,7]. This implies a link between cell cycle regulation and metabolic processes [8]. Indeed the following cell cycle regulators, such as the transcription factor E2Fs and the G1 factors p21, p27, cyclin D3 and cyclin dependent kinase 4 have been shown to regulate MCE and to contribute to adipogenesis by inducing

Abbreviations: MCE, mitotic clonal expansion; C/EBP, CCAAT/enhancer-binding protein; PPARγ, peroxisome proliferator-activated receptor γ; IR, insulin receptor; PI3K, phosphoinositide 3-kinase; PKB, protein kinase B; Topo IIα and β, DNA Topoisomerase IIα and β; mTOR, mammalian target of rapamycin; IBMX, 3-isobutyl-2-methylxanthine; PARP, Poly(ADP-ribose) Polymerase; PFA, paraformaldehyde; PCH, pericentromeric chromatin.

* Corresponding author at: Department of Molecular Biology, University of Bergen, Høyteknologisenteret, Thormølensgate 55, 5008 Bergen, Norway.
E-mail address: aurelia.lewis@uib.no (A.E. Lewis).

http://dx.doi.org/10.1016/j.cellsig.2016.07.002

the transcription or by facilitating the transcriptional activity of PPARγ [9–11]. Consistently, inhibition of DNA synthesis blocks both MCE and adipogenesis [4] by preventing the production of a PPARγ ligand prior to the optimal transcriptional activation of PPARγ [12]. Although numerous studies have clearly shown that MCE is required for adipogenesis, the underlying molecular mechanisms triggering MCE are however not fully understood.

Adipocytes respond to insulin by activating the insulin receptor (IR), the phosphorylation of IR substrates and the activation of the class I phosphoinositide 3-kinase (PI3K) signalling pathway, which ultimately leads to the transcription of specific insulin responsive gene products and regulation of glucose and lipid homeostasis [13–15]. Activation of class I PI3K generates the polyphosphoinositide lipid product phosphatidylinositol(3,4,5) triphosphate (PtdIns(3,4,5)P_3), which is responsible for the activation of protein kinase B (PKB)/Akt in 3T3-L1 cells [16]. PKB/Akt is activated by sequential phosphorylation on Thr308 and Ser473 by 3-phosphoinositide-dependent protein kinase-1 (PDK1) and mammalian target of rapamycin (mTOR) complex 2 respectively [17,18]. Activated Akt can translocate to different intracellular sites where it phosphorylates a myriad of substrates. When in the nucleus, PKB/Akt phosphorylates and inactivates the transcription factor FoxO1 by nuclear exclusion, thus permitting adipogenic gene transcription [19]. The PI3K-PKB/Akt pathway is known to be essential for adipogenesis [20–24] and PI3K inhibition was shown to prevent MCE in 3T3-L1 cells [21,25], but the underlying molecular mechanisms linking the activation of the PI3K pathway and the induction of MCE are unclear.

DNA topoisomerases are a family of enzymes that resolve DNA topological features such as catenation and supercoiling, arising during DNA replication, transcription and sister chromatid entanglement during mitosis [26,27]. DNA topoisomerases consist of two classes, type I and type II which catalyse single and double strand breaks respectively. Mammalian cells express two type II isoforms (Topo IIα and β) that are encoded by different genes. They both have the same catalytic activity but have different expression patterns during cell division and distinct cellular functions [26,28]. Topo IIα is expressed in dividing and pluripotent cells while Topo IIβ is found in post-mitotic and differentiating cells. Topo IIα is highly expressed in actively dividing cells whereas Topo IIβ is more abundant in terminally differentiated cells [29–32]. The level of Topo IIα expression varies during cell-cycle progression with lowest levels observed in G1 followed by a steady increase peaking at the G2 and M phases of the cell cycle [33–35]. Topo IIβ expression levels vary less than Topo IIα throughout the cell cycle and either remain constant or decrease [33,35]. In light of this, we hypothesised that Topo II, in particular Topo IIα, may participate in MCE and adipocyte differentiation. We have now shown that Topo IIα levels are up-regulated in the early steps of adipocyte differentiation in a PI3K/mTOR-dependent manner. The precise increase of Topo IIα coincides with the time frame of occurrence of MCE and that its activity contributes to MCE and is thus required for adipocyte differentiation.

2. Materials and methods

2.1. Reagents

Calf serum, dexamethasone, dexrazoxane (ICRF-187), Dulbecco's Modified Eagles Medium (DMEM), dimethylsulfoxide (DMSO), fetal bovine serum (FBS), IBMX, insulin, LY294002, Oil Red O, Mammalian Protease Inhibitor Cocktail, penicillin/streptomycin and rapamycin were from Sigma-Aldrich. Benzonase was from Merck Millipore. The PI3K selective inhibitors targeting p110α (A66) and p110β (TGX-221) were from Selleck Chemicals and p110δ (PI3065) from Cayman Chemical respectively. The following antibodies were used: anti-PI3K p110α (4249), anti-Poly(ADP-ribose) Polymerase (PARP) (9542), anti-ribosomal protein S6 (2217) and anti-phospho-S240/S244 ribosomal protein S6 (5364) from Cell Signaling Technology; anti-DNA Topoisomerase IIα (ab52934) from Abcam; anti-PPARγ (MA5-14889) from ThermoFisher; anti-DNA Topoisomerase IIβ (HPA024120) from Sigma-Aldrich and anti-β-Actin (sc-69879), anti-PI3K p110β (IgM, sc-376492), anti-PI3K p110δ (sc-7176), anti-cyclin A (sc-596) from Santa Cruz Biotechnology. Hoechst, goat anti-mouse/rabbit conjugated with horseradish peroxidase (HRP) and Alexa 488-conjugated secondary antibodies were from Life Technologies. HRP-conjugated goat anti-mouse IgM was from Abcam. TO-PRO-3 nucleic acid stain (T3605) and Prolong Gold antifade reagent (p36930) for mounting were from Thermo Fisher scientific.

2.2. Cell culture and differentiation of 3T3-L1 cells

3T3-L1 fibroblasts were kindly provided by Lise Madsen (University of Copenhagen, Denmark) cultured in high-glucose DMEM supplemented with 10% calf serum and 100 units/ml penicillin and 100 μg/ml streptomycin and maintained at about 70% confluence. To induce differentiation, cells were grown to confluence. At two-three days post confluency (day 0), 3T3-L1 cells were incubated with a differentiation cocktail (abbreviated MDI) containing 500 μM IBMX, 250 nM dexamethasone and 5 μg/ml insulin in DMEM with 10% FBS and antibiotics for 2 days. After 2 days (day 2), the differentiation medium was removed and the cells were incubated in DMEM-10% FBS and antibiotics containing 5 μg/ml insulin (insulin medium) for 2 more days. At day 4 and 6 the medium was changed to DMEM-10% FBS and antibiotics. Adipocyte differentiation was verified for each thawed batch of cells by Oil Red O staining at day 0 and day 7. For PI3K and rapamycin inhibitor experiments, 3T3-L1 cells were pre-incubated on day 0 for 1 h with inhibitors or DMSO before the addition of the MDI medium containing inhibitors or DMSO as well as before the addition of the insulin medium on day 2. Inhibitors were not added onwards from day 4. Cells were then either lysed on day 1 or stained with Oil Red O on day 7. For Topoisomerase II inhibitor treatments, 50 μg/ml of ICRF-187 or equal volume of DMSO was added to the MDI medium on day 0 and with the insulin medium on day 2 and not thereafter. Cells were either lysed for Western immunoblotting on day 3 or stained with Oil Red O on day 7. For treatments from days 0–2 or 3–5, 50 μg/ml of ICRF-187 or equal volume of DMSO was added either with the MDI medium on day 0 or directly into existing insulin medium on day 3. Insulin medium was then changed to DMEM-10% FBS and antibiotics on day 5 rather than day 4 and no ICRF-187 was added from this point onwards. This gave a total of 2 days of exposure to the inhibitor or DMSO (days 0–2 or 3–5). Cells were then either lysed for Western immunoblotting on day 5 or stained with Oil Red O on day 7.

2.3. Oil Red O staining

On day 0 or 7 the cells were washed twice with PBS and fixed with 3.7% paraformaldehyde (PFA) for 15 min at room temperature. Cells were stained with 0.3% Oil Red O in 60% isopropanol working solution for 1 h at room temperature and washed 5 times with MilliQ H_2O. The plates were left to dry at room temperature and stored at 4 °C. For quantification, Oil Red O was dissolved with isopropanol and the absorbance was measured at 500 nm.

2.4. SDS-PAGE and Western immunoblotting

Cells were washed with cold PBS and lysed in RIPA lysis buffer (50 mM Tris pH 8.0, 0.5% deoxycholic acid, 150 mM NaCl, 1% NP-40, 0.1% SDS) supplemented with 5 mM NaF, 2 mM Na_3VO_4 and 1× Protease Inhibitor Cocktail and sonicated in an ultrasonic bath for 1–2 min or incubated with 16 U benzonase (for 35 mm plates) for 30 min on ice. Excess lipids were removed (day 5 and 7 usually). Protein concentration was determined using BCA reagents (Pierce) and equal amount of proteins (40–50 μg) were resolved by SDS-PAGE and transferred to nitrocellulose membranes. Membranes were blocked in 7% fat-free milk in TBS-T (50 mM Tris pH 7.5, 150 mM NaCl, 0.1% Tween-20) for 1 h at

room temperature and incubated overnight at 4 °C with primary antibodies and subsequently with secondary antibodies conjugated to HRP for 1 h at room temperature. Protein detection was performed by enhanced chemiluminescence (ECL) using the SuperSignal West Pico or Femto Chemiluminescent Substrate (Pierce) and detected with a BioRad ChemiDoc™ Xrs+. The membranes were stripped for 20 min at RT in Restore™ Western Blot Stripping Buffer (Pierce), washed in TBS-T, blocked again and probed with the corresponding secondary antibody to detect any remaining signal prior to further immunoblotting when required. Equal protein loading was confirmed by immunodetection of β-actin. Protein bands were quantified using ImageJ and normalised to β-actin and then to control.

2.5. Immunofluorescence staining

3T3-L1 cells, seeded on 12 mm coverslips, were incubated with the MDI medium at day 0. Cells were fixed with 3.7% paraformaldehyde for 10 min at room temperature, washed twice with PBS, permeabilised with 0.25% Triton X-100 in PBS for 10 min and blocked for 1 h with blocking buffer (3% fatty-acid free BSA in PBS-T). The cells were incubated overnight at room temperature with anti-Topo IIα or anti-Topo IIβ antibodies diluted at 1:100 in blocking buffer, followed by incubation with anti-rabbit IgG antibody conjugated to Alexa-488 diluted in blocking buffer (1:200) for 1 h at room temperature. Washes were performed with 0.05% PBS-T after antibody incubations. The coverslips were stained for 20 min at room temperature with TO-PRO-3 nucleic acid stain before mounting. Control staining with secondary antibody alone under the same staining and exposure conditions showed no staining. Images were acquired with a Leica TCS SP5 confocal laser scanning microscope equipped with a 63×/1.4 oil immersion lens and using 488 nm and 633 nm laser lines. Images were processed with the Leica application suite version 4.4.

2.6. EdU staining

EdU staining was performed according to the Invitrogen's Click-iT EdU imaging kit (C10339). 3T3-L1 cells were seeded on 12 mm coverslips. 2–3 days after reaching confluency, cells were incubated with MDI medium containing either 50 μg/ml ICRF-187 or DMSO for 1 or 2 days. Cells were incubated with 10 μM EdU for the last 2 h prior fixation. Cells were fixed for 15 min at room temperature in 3.7% PFA on days 0, 1 and 2. EdU was stained for 30 min with Alex-594 according to the kit protocols (except buffer reaction additive was prepared as 10 × 500 mM ascorbic acid in H_20). Cells were then blocked for 1 h at room temperature in 3% BSA, 0.1% Triton X-100 in PBS before incubation with anti-Topo IIα (1:100) and subsequently with anti-mouse IgG secondary antibody conjugated to Alexa-488 (1:200) in blocking buffer for 1 h at room temperature. Washes were performed with 0.05% PBS-T after each antibody incubation. DNA staining was then done using Hoechst for 30 min at room temperature before mounting. Images were acquired with a Leica DMI6000B fluorescence microscope using a 40× objective.

3. Results

3.1. DNA Topoisomerase IIα is transiently expressed during 3T3-L1 preadipocyte differentiation in a PI3K-dependent manner

To investigate whether Topo IIα and/or β play a role in the mitotic clonal expansion occurring during the early stages of adipocyte differentiation, we first evaluated the expression levels of each isoform upon stimulation of 3T3-L1 cells with the differentiation cocktail for the first 3 days and up to 7 days (Fig. 1A). The expression levels of both isoforms were distinct throughout the time course. Topo IIα was undetectable in post-confluent cells (day 0), but its expression increased within 16 h of stimulation and peaked at day 1, which correlated with an increase in expression of cyclin A. The expression levels of Topo IIα then declined from day 2. The decrease in Topo IIα coincided with an increase in PPARγ2 expression. In contrast, Topo IIβ was present in post-confluent cells as well as throughout adipogenesis. The levels of Topo IIβ varied between experiments showing either an increase from day 0 to day 1 (Fig. 1A) or constant levels throughout the time course (Fig. 1E and Supplementary Fig. S1). The pattern of protein expression of both isoforms is consistent with the reported transcript levels by Mikkelsen *et al.* [36] (Supplementary Fig. S2) and for Topo IIα by Soukas *et al.* [37]. In immunostaining analyses, we showed that, similarly to Western analyses, a great increase in cells stained for Topo IIα at day 1 compared to day 0, whereas the majority of cells in both day 0 and day 1 stained for Topo IIβ (Fig. 1B). In addition, Topo IIα exhibited two different patterns of localisation, either diffuse throughout the nucleus or in foci strongly stained by the DNA dye TO-PRO-3 and known as centric/pericentric heterochromatin (PCH) [38]. The localisation pattern of Topo IIβ was mostly diffuse with occasional cells with a punctate pattern but it did not change overall between day 0 and 1 (Fig. 1B). Since the differentiation of 3T3-L1 cells has been shown be dependent on the PI3K pathway [21,23,25,39], we investigated the effect of the pan-PI3K inhibitor, LY294002, on the protein levels of Topo IIα and β upon differentiation at day 1. Consistent with other studies, inhibition of PI3K with LY294002 greatly reduced the storage of triglycerides (Fig. 1C–D). Interestingly, the protein levels of Topo IIα detected at day 1 were also consistently reduced by the addition of LY294002 (Fig. 1E–F). However, the effects of PI3K inhibition on Topo IIβ expression were a lot more variable with the addition of LY294002 (Fig. 1E–F), depending on the level detected in day 1. We monitored the activity of the PI3K pathway by analysing the levels of phospho-S240/S244 of the 40S ribosomal protein S6 (pRS6). As expected, the levels of pRS6 were elevated at day 1 and were then decreased following PI3K inhibition while total RS6 levels remained unchanged (Fig. 1E).

3.2. All class IA PI3K catalytic isoforms are expressed in 3T3-L1 cells during differentiation but selective inhibition of p110α reduces differentiation and DNA Topoisomerase IIα

The PI3K class IA family of enzymes consists of the catalytic subunits p110α, p110β and p110δ and the expression pattern of each isoform was investigated upon adipocyte differentiation. p110α, β and δ were all expressed and their levels remained relatively stable throughout the time course (Fig. 2A). We therefore sought to determine which PI3K isoforms contribute to adipogenesis as well as the regulation of the levels of Topo IIα using the selective inhibitors A66 (p110α), TGX-221 (p110β) and PI3065 (p110δ). Addition of A66 reduced the storage of triglycerides dose-dependently reaching the same levels obtained by LY294002 addition at the highest concentration of A66 (10 μM) (Fig. 2B–C). PI3065 had little effect at 0.1 or 1 μM but greatly decreased triglyceride storage at the highest concentration of 10 μM. In contrast TGX-221 had the least effect of all 3 inhibitors. The levels of Topo IIα were also affected by the addition of these PI3K inhibitors with most effect seen at higher doses of A66 (1 and 10 μM), TGX (10 μM) and PI3065 (10 μM) reflecting the results obtained for the effects of inhibitors on storage of triglycerides (Fig. 2D–E).

3.3. mTOR regulates the protein levels of DNA Topoisomerase IIα

mTOR, which is known to control protein synthesis, is also reported to contribute to adipogenesis [39,40] and we therefore evaluated the effect of rapamycin, an inhibitor of mTOR, on triglyceride storage and Topo IIα protein expression (Fig. 3). Rapamycin dramatically lowered the deposition of triglycerides at concentrations as low as 1 nM (Fig. 3A–B). Accordingly, the expression levels of Topo IIα also decreased with the addition of rapamycin (Fig. 3C–D), showing therefore a role for the PI3K/mTOR pathway in regulation Topo IIα protein synthesis.

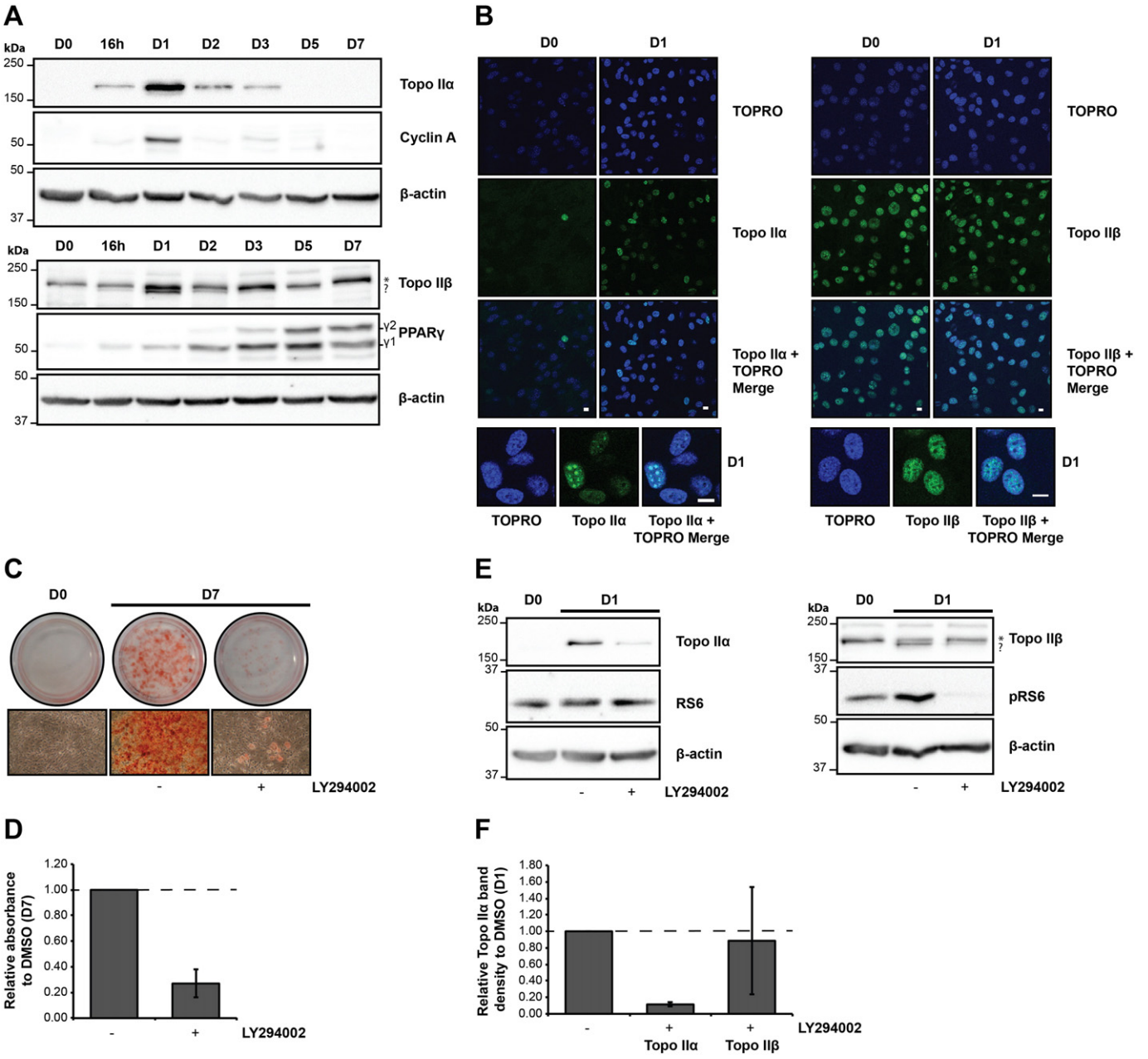

Fig. 1. Expression profile of Topo IIα and β during adipocyte differentiation of 3T3-L1 cells and effect of pan-PI3K inhibition on their expression. A. Representative Western blots of 3T3-L1 cells whole cell extracts, obtained at day 0 (D0) and up to 7 days of differentiation (D7), probed with anti-Topo IIα, anti-Topo IIβ, anti-cyclin A, anti-PPARγ and anti-β-actin as a loading control. B. Immunostaining of 3T3-L1 cells fixed at day 0 and day 1 with anti-Topo IIα and β and nuclear counterstained with TOPRO. Lower panels show magnified examples, scale bar indicates 10 μm (63×). C. Representative photos of 3T3-L1 cells fixed and stained with Oil Red O on day 0 (D0) or day 7 (D7) of differentiation in the presence of 10 μM LY294002 (+) or DMSO (−) for the first 4 days (photos of plates on top, microscope 10× magnification on bottom), D. Quantification of Oil Red O staining from day 7 (D7) relative to DMSO control (−). E. Representative Western blots of 3T3-L1 whole cell extracts obtained at day 0 (D0) or day 1 (D1) of differentiation after incubation with 10 μM LY294002 (+) or DMSO (−), probed with anti-Topo IIα, anti-Topo IIβ, anti-ribosomal protein S6 (RS6), anti-phospho-S240/S244-ribosomal protein S6 (pRS6) and β-actin as loading control, F. Quantification of Topo IIα and Topo IIβ protein band densitometry (top band only (*)) from day 1 (D1) normalised to β-actin and then to DMSO control (−). All quantifications are from 5 independent experiments, shown as mean ± SDs. Bands of interest on Western blots are highlighted with * if multiple.

3.4. DNA Topoisomerase II activity is required for adipocyte differentiation and PPARγ1/2 up-regulation

Topoisomerase II inhibition with merbarone has previously been shown to reduce the transcription of PPARγ2 and several PPARγ2-dependent genes in 3T3-L1 cells at later stages of differentiation *via* the inhibition of PARP1 (ARTD1) [41,42]. To further evaluate Topoisomerase II activity requirement in adipocyte differentiation, post-confluent 3T3-L1 cells were incubated with the Topoisomerase II inhibitor, ICRF-187. Inhibition of topoisomerase II resulted in a decrease in both stored triglycerides (Fig. 4A–B) and PPARγ1 and 2 protein levels (Fig. 4C–D). Considering that the levels of Topo IIα decrease from day 2 of stimulation but Topo IIβ remains present throughout the time course (Fig. 1A), 3T3-L1 cells were differentiated in the presence of ICRF-187 either for the first 2 days or days 3–5 to elucidate the requirement of Topo II in early or late differentiation phases. Addition of ICRF-187 at the start of differentiation for days 0–2 resulted in a greater decrease in the amount of stored triglycerides than when added later at days 3–5 (Fig. 4E–F). This was reflected with a greater decrease in the levels of PPARγ1 and 2 when cells were treated early at days 0 and 2, compared to later treatments at days 3–5 (Fig. 4G–H) when the levels of Topo IIα have greatly declined (Fig. 1A). To verify that the effect of topoisomerase inhibition

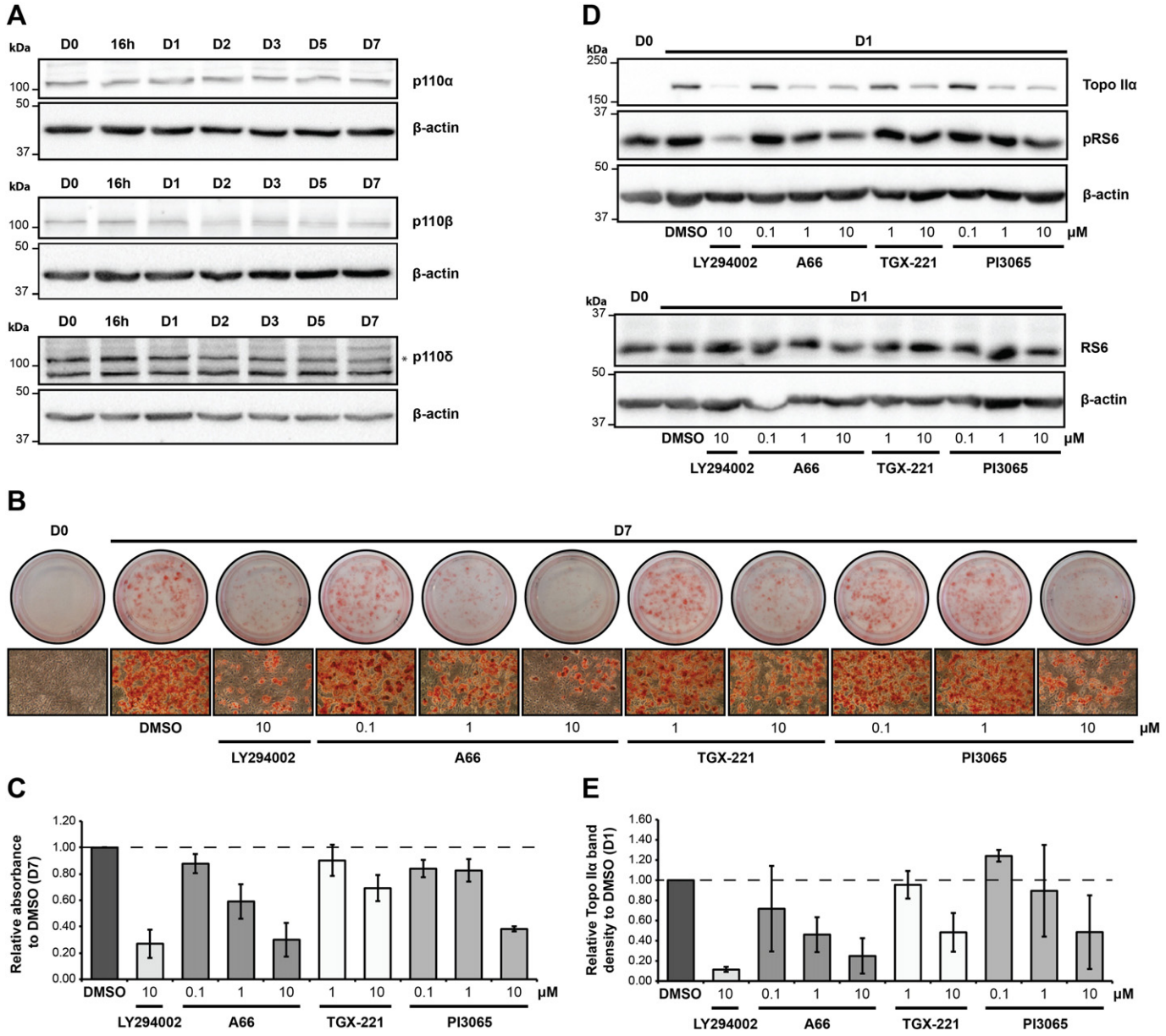

Fig. 2. Expression levels of class IA PI3K catalytic isoforms during differentiation and effect of their selective inhibition on differentiation and Topo IIα expression. A. Representative Western blots of whole cell extracts from 3T3-L1 cells, day 0 (D0) and up to 7 days (D7) of differentiation, blots probed with anti-PI3K p110α, β, δ and anti-β-actin as a loading control. B. Representative photos of 3T3-L1 cells fixed and stained with Oil Red O on day 0 (D0) or day 7 (D7) of differentiation after incubation for the first 4 days with the selective PI3K inhibitors for p110α (A66), p110β (TGX-221) or p110δ (PI3065), LY294002 or DMSO (photos of plates on top, microscope 10× magnification on bottom), C. Quantification of Oil Red O staining from day 7 (D7) plates normalised to DMSO. D. Representative Western blots of 3T3-L1 whole cell extracts obtained at day 0 (D0) or day 1 (D1) of differentiation in the presence of PI3K inhibitors or DMSO, probed with anti-Topo IIα, anti-ribosomal protein S6 (RS6), anti-phosphoS240/S244-ribosomal protein S6 (pRS6) and β-actin as loading control, E. Quantification of Topo IIα protein band densitometry from day 1 (D1) normalised to β-actin and then to DMSO. All quantifications were from a minimum of 2–3 independent experiments, shown as means ± SDs. Bands of interest on Western blots are highlighted with * if multiple.

was not due to an induction of cell death, we monitored PARP cleavage under the same conditions. The PARP levels were increased at day 3 (Fig. 4C) and day 5 (Fig. 4G) but we could not detect any PARP cleavage.

3.5. DNA Topoisomerase IIα activity contributes to cell proliferation, but not DNA synthesis, during MCE

Since Topo II inhibition has a greatest effect on adipocyte differentiation when used during the first 2 days (Fig. 4E–H) and since Topo IIα is transiently expressed in the early stages of differentiation (Fig. 1A), we wondered if Topo IIα played a role in the MCE phase. We first assessed the effect of ICRF-187 on DNA synthesis using EdU staining. A large increase in the number of Topo IIα-positive cells was seen at day 1 compared to day 0 (from 2.0 ± 1.4 to 47.8 ± 5.4%), and on average about half of these cells at day 1 were also labelled with EdU (Fig. 5A–B). In all conditions, most cells labelled with EdU were also Topo IIα-positive and on average less than 1% of cells were both EdU-positive and Topo IIα-negative. At day 2, the number of Topo IIα-positive cells decreased slightly and only a small proportion of these cells were also EdU-positive (4.0 ± 2.1%), compared to day 1. Addition of ICRF-187 to 3T3-L1 cells did not significantly affect the number of EdU-positive cells at day 1 but a slight decrease was apparent at day 2 of differentiation (Fig. 5A–B). Moreover, the number of Topo IIα-positive cells remained elevated in ICRF-187-treated cells at day 2, perhaps owing to the mode of action of the inhibitor clamping Topo IIα to DNA and thus maybe preventing its release from DNA and its degradation [43–45] (Fig. 5A–B). We have shown that Topo IIα has two different distribution patterns in the nucleus at day 1, *i.e.* either diffuse or concentrated in

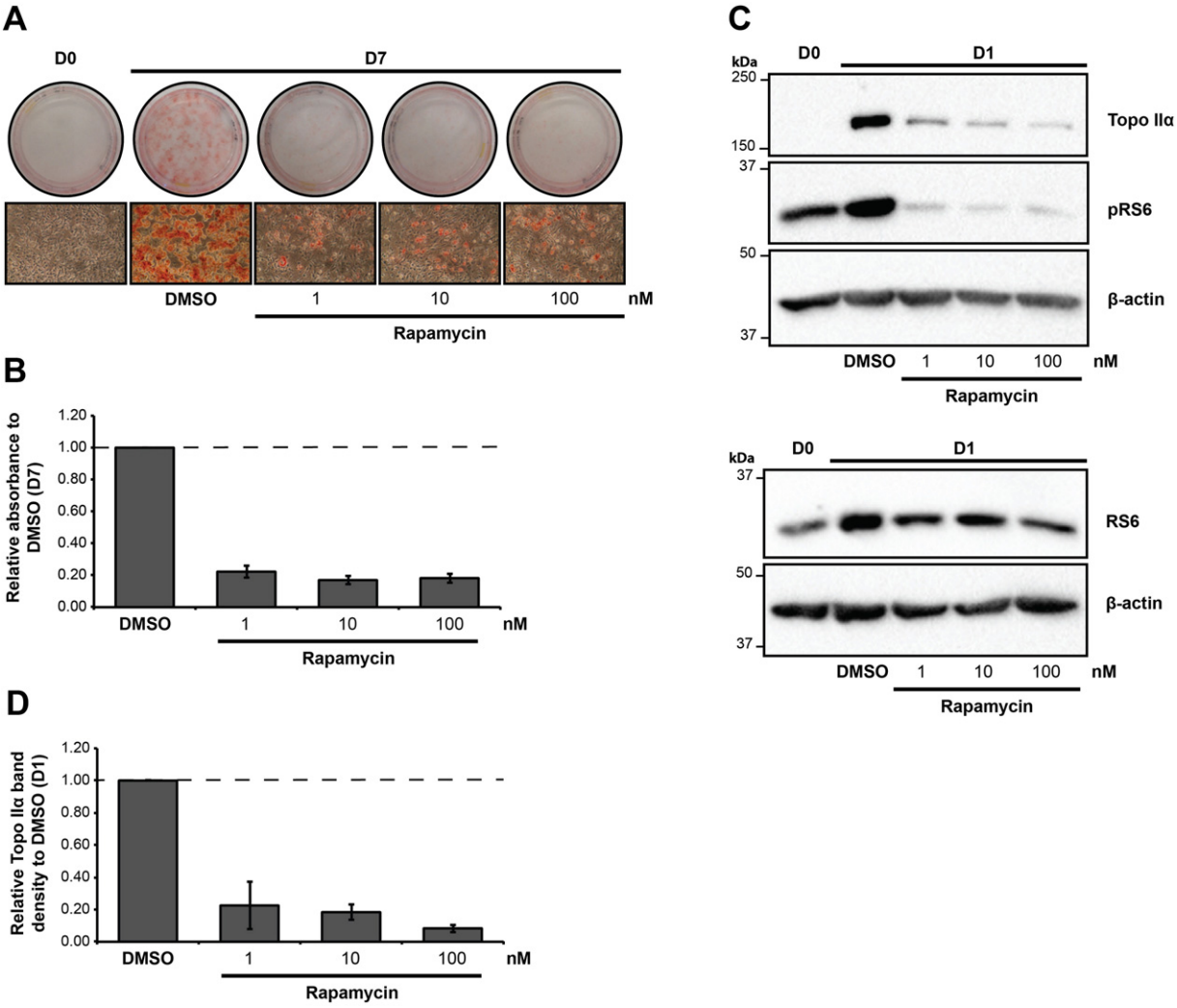

Fig. 3. mTOR controls the protein levels of Topo IIα. A. Representative photos of 3T3-L1 cell plates fixed and stained with Oil Red O stain on day 0 (D0) or day 7 (D7) of differentiation after incubation for the first 4 days with rapamycin or equivalent volume DMSO (photos of plates on top, microscope 10× magnification on bottom), B. Oil Red O from day 7 (D7) plates was then extracted and quantified, relative absorbance normalised to DMSO control. C. Representative Western blot of 3T3-L1 whole cell extracts on day 0 (D0) or on day 1 (D1) of differentiation after incubation with rapamycin or equivalent volume DMSO, probed with anti-Topo IIα, anti-ribosomal protein S6 (RPS6), anti-phosphoS240/S244-ribosomal protein S6 (pRS6) and β-actin as loading control, D. Quantification of Topo IIα protein band densitometry from day 1 (D1) normalised to β-actin and then to DMSO. All quantifications are from 3 independent experiments, shown graphs as mean ± SD.

DNA-stain rich foci known as PCH (Fig. 1B). The PCH/diffuse staining ratio was of 0.76 on day 1 and of 0.89 on day 2 (Fig. 5C). ICRF-187 treatment caused the ratio to increase on both day 1 and 2 compared to untreated cells to 6.6 and 3.1 respectively (Fig. 5C). The increase in the proportion of cells stained with Topo IIα in PCH may again most likely be due to the mode of action of the inhibitor and may suggest that Topo IIα is particularly active at PCH at the very early stages of adipocyte differentiation (Fig. 5C). In addition Topo IIα co-stains often with EdU at these sites (Fig. 5A), which may indicate that Topo IIα participates in DNA synthesis of PCH. In sum, Topo II inhibition had no effect or very little on DNA synthesis on both day 1 and 2 of differentiation. We therefore analysed the relative cell numbers under the same conditions and showed a decrease in the relative cell number in ICRF-187-treated cells on day 2 compared to DMSO-treated cells (Fig. 5D).

4. Discussion

Cell division, also specifically known as MCE, is thought to be a prerequisite for adipocyte differentiation [4,5]. Entry into S phase and DNA synthesis have been shown to be particularly important [46]. In this report, we provide evidence that Topo II activity is required for pre-adipocyte differentiation, acting notably at the early steps during MCE. This is supported by the following results. Firstly, when Topo II is inhibited prior to the onset of MCE, *i.e.* from days 0 to 2, the effect on differentiation was greatest compared to later inhibition at days 3–5. Secondly, the levels of Topo IIα are transiently induced during differentiation and peak at day 1 when DNA synthesis and cyclin A, an S phase indicator, are highest. Finally, cells that are in S phase at day 1 almost all stain for Topo IIα. More specifically, Topo IIα localises to sites of DNA replication at day 1. In contrast, the expression and localisation of Topo IIβ does not tend to correlate with S phase. Our findings would hence point to a role for Topo IIα at this stage of differentiation. The contribution of Topo IIβ to MCE cannot be excluded however as it is expressed throughout differentiation and thus its expression overlaps with that of Topo IIα. Moreover, ICRF-187, which was used in this study, is thought to target both Topo IIα and Topo IIβ [43], although another study showed that the activity of Topo IIα may be more affected than Topo IIβ by ICRF-187 in HeLa cells due to increased retention to DNA [47].

In this study, we have observed that Topo IIα localises to intense DNA-stained areas at day 1, also known as chromocenters, consisting of centromeric and pericentromeric heterochromatin, which are particularly prominent in murine cells [38,48]. Similarly, the transcription factor CCAAT/enhancer-binding proteins β and δ (C/EBPβ and δ) were reported to show the same pattern by interacting with satellite DNA

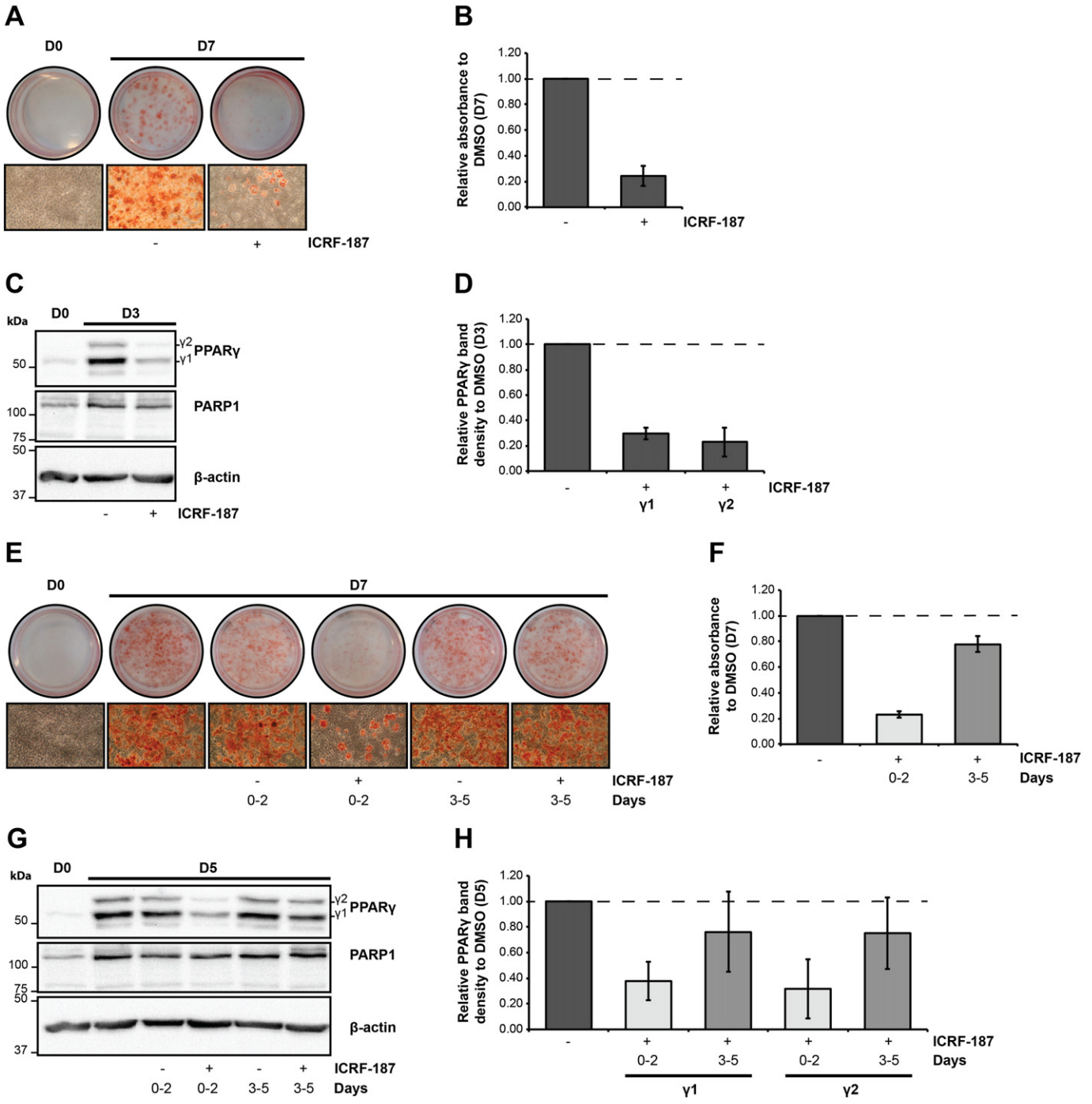

Fig. 4. Topo II activity is required for adipocyte differentiation and PPARγ1 and 2 up-regulation. A. Representative photos of 3T3-L1 cells fixed and stained with Oil Red O on day 0 (D0) and day 7 (D7) of differentiation after incubation with 50 μg/ml of Topoisomerase II inhibitor ICRF-187 (+) or equivalent volume of DMSO (−) for the first 4 days (photos of plates on top, microscope 10× magnification on bottom), B. Quantification of Oil Red O staining from day 7 (D7) normalised to DMSO (−). C. Representative Western blots of 3T3-L1 whole cell extracts on day 0 (D0) or on day 3 (D3) of differentiation after incubation with 50 μg/ml of ICRF-187 (+) or DMSO (−) for the first 3 days of differentiation, probed with anti-PPARγ, anti-PARP and β-actin as a loading control, D. Quantification of PPARγ1 and 2 protein bands from day 3 (D3) normalised to β-actin and then to DMSO (−). E. Representative photos of 3T3-L1 cells fixed and stained with Oil Red O on day 0 (D0) and day 7 (D7) of differentiation after incubation 50 μg/ml of ICRF-187 (+) or DMSO (−) for days 0–2 or 3–5 (photos of plates on top, microscope 10× magnification on bottom), F. Quantification of Oil Red O staining from day 7 (D7) normalised to DMSO control (−). G. Representative Western blots of 3T3-L1 whole cell extracts obtained on day 0 (D0) or on day 5 (D5) of differentiation after incubation with 50 μg/ml of ICRF-187 (+) or DMSO (−) for days 0–2 or 3–5, probed with anti-PPARγ, anti-PARP and β-actin as a loading control, H. PPARγ1 and 2 from day 5 (D5) of Western blots were then quantified, relative band density was normalised to β-actin and then to DMSO (−). All quantifications are calculated from a minimum of 3 independent experiments, shown as means ± SDs.

in centromeric heterochromatin from 12 to 16 h of induction of differentiation and concomitantly with DNA synthesis [48]. Tang and Lane [48] suggest that the association of C/EBPβ and δ with centromeric heterochromatin is functionally important for the regulation of MCE as this may delay their acquisition of DNA binding activity and hence the transcription of C/EBPα and PPARγ. Considering that C/EBPα is a mitotic repressor, the delayed expression of C/EBPα is hence thought to ensure the completion of MCE [49]. In addition, C/EBPβ has been shown to induce the transient expression of the methyl transferase G9a during MCE, which leads to histone H3K9 dimethylation on the promoters of C/EBPα and PPARγ and their repression [50]. In our study, we show that Topo II inhibition with the addition of ICRF-187 caused a higher

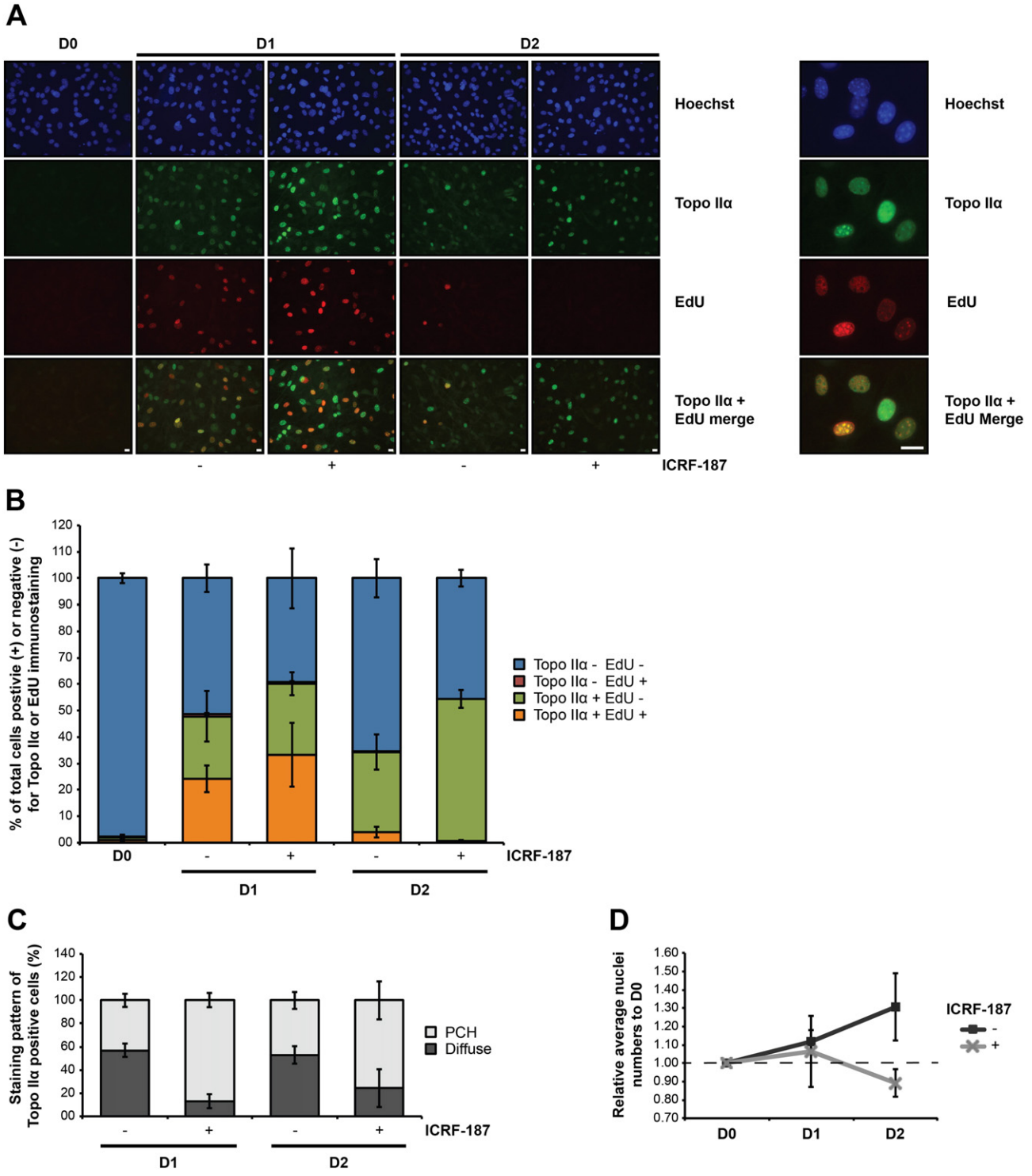

Fig. 5. Topo IIα activity during mitotic clonal expansion phase of adipogenesis. A. EdU labelling and Topo IIα immunostaining of 3T3-L1 cells on days 0 (D0), 1 (D1) and 2 (D2) of differentiation in the presence of 50 μg/ml of ICRF-187 (+) or DMSO (−), nuclear counterstained with Hoechst, Side panels are magnified examples of Topo IIα and EdU staining from day 1 with DMSO control, scale bar indicates 10 μm (40×). B. Quantification of 3T3-L1 cells positive for Topo IIα and EdU (Topo IIα+ EdU+, orange), Topo IIα only (Topo IIα+ EdU−, green), EdU only (Topo IIα− EdU+, red) or neither Topo IIα nor EdU (Topo IIα− EdU−, blue) on day 0 (D0), 1 (D1) and 2 (D2) in the presence of 50 μg/ml of ICRF-187 (+) or DMSO (−). At least 300 3T3-L1 cells were counted from a minimum of 5 different 40× fields per experiment. C. Quantification of staining patterns of Topo IIα, categorised as either pericentromeric heterochromatin (PCH) or diffuse. The percentages are calculated from total number of Topo IIα positive cells for each condition per experiment. D. Quantification of relative nuclei numbers on day 1 (D1) and 2 (D2) of 3T3-L1 cells treated with 50 μg/ml of ICRF-187 (+) or DMSO (−). Nuclei were counted from a minimum of 5 different 40× fields per experiment and the average number of Hoechst-stained nuclei per field was normalised to day 0 (D0). All quantifications calculated from 3 independent experiments, graphs shown as mean ± SD.

percentage of cells displaying this pattern, perhaps due to the mode of action of the inhibitor. ICRF-187 is a member of the bisdioxopiperazines class of Topo II catalytic inhibitors, which are known to trap Topo II on DNA as a protein-DNA clamp [43–45]. DNA-trapped Topo IIα may indicate the sites of Topo IIα activity, which are particularly noticeable in heterochromatin, consistent with a study in human cells by Agostinho et al. [47]. Topo IIα may therefore have a role in the replication of heterochromatin. However our study did not uncover a role for

Topo II in DNA synthesis since its inhibition with ICRF-187 led to a small increase in EdU labelling at day 1 rather than a decrease, which was mirrored by a slight increase in cyclin A (data not shown). These results may instead be indicative of a delay in the progression of DNA replication. Consistently, Topo IIα inhibition with another bisdioxopiperazine Topo II catalytic inhibitor, ICRF-193, in *Xenopus* sperm nuclei did not alter entry into S phase and DNA synthesis but delayed the completion of DNA replication [51] due to the perturbation of chromatin structure [52]. The localisation of Topo IIα to chromocenters or centromeric chromatin has previously been reported [47,53] and shown to play a role correlated to the accurate segregation of chromatids in anaphase [54]. In line with this, Topo inhibition with ICRF-187 has been shown to cause the incomplete segregation of chromosomes [55]. These reports would hence support a role for Topo IIα at the centromeres during mitosis of 3T3-L1 pre-adipocytes. Consistently, we showed that ICRF-187 induced a decrease in the average number of cells at day 2. In addition, DNA-trapped Topo IIα may be stable and may prevent its degradation, as shown in other studies using ICRF-193 [56,57], and this might explain why the number of Topo IIα positive cells remains high in day 2 with ICRF-187 compared to the overall decreased protein levels detected by immunoblotting at day 2 without the inhibitor.

Previous studies in 3T3-L1 cells showed that Topo II activity is necessary for PARP1 (alias ARTD1) activation and the recruitment of PARP1 to PPARγ response elements (PPREs) of PPARγ-dependent adipogenic genes and therefore for their subsequent expression and adipocyte differentiation [41,42]. However, these studies showed a later contribution for Topo II-dependent PARP1 activity and PARP1 recruitment to PPREs which were demonstrated at day 7 (equivalent to day 5 in our study) in cells treated with an inhibitor of Topo II at days 4/5–6 (equivalent to days 2/3–4 in our study). In light of our results, inhibition of Topo II at these time points would more likely target Topo IIβ rather than Topo IIα, since its expression is still detectable, and points therefore to a role for Topo IIβ in the regulation of PARP1 mediated adipogenic gene expression at these time points. Topo IIβ and PARP1 have indeed been shown to be part of the same protein complex and to be important in activating transcription *via* the local formation of dsDNA breaks in a number of other studies [58–60]. Consistently, a role for Topo IIβ in transcription linked to cell differentiation is supported in another study showing the recruitment of Topo IIβ along with PARP1 on the fatty acid synthase (FAS) promoter in hepatocytes responding to insulin during lipogenesis [61]. Therefore, Topo IIβ may also contribute since it is expressed continually throughout differentiation. Both isoforms may hence operate catalytically similarly but on different genomic sites and times of differentiation since they appear to be targeted to different nuclear sites, as detected by immunostaining.

It is well known that the addition of pan PI3K inhibitors such as LY294002 or wortmannin inhibits adipogenesis in 3T3-L1 cells [21,23,25,39,62]. Rapamycin, an inhibitor of mTOR, has also been shown to inhibit the differentiation of 3T3-L1 cells by inhibiting MCE [39,40] and Rb protein phosphorylation [39]. Our studies confirmed the effect of PI3K and mTOR inhibition on adipogenesis using LY294002 and rapamycin. We also showed that this was accompanied by reduced expression of Topo IIα, indicating that the PI3K/mTOR pathway regulates the expression of Topo IIα during MCE in these cells. The expression of Topo IIβ exhibited a lot of variations but did not seem to be regulated by the PI3K pathway.

Since LY294002 is a pan-PI3K inhibitor we wondered if the effect seen on differentiation and expression of Topo IIα could be attributed to a particular PI3K class IA catalytic subunit isoform. We find that 3T3-L1 cells express all class IA PI3K catalytic isoforms, *i.e.* p110α, β and δ, and that their expression levels remain relatively constant during the differentiation time course. Previous reports showed some slight variations in the levels of these isoforms in 3T3-L1 cells during differentiation, *i.e.* showing an increase in p110β [63], or an increase in p110α levels and a decrease in p110δ [23]. These slight differences may be longer differentiation protocol for up to 9 days [23]. Using selective inhibitors, our study shows that p110α and p110δ, to a lesser extent, are required for adipocyte differentiation. The major contribution of p110α in adipogenesis is in agreement with the study of Kim, Shepherd and Chaussade [23] using a different selective inhibitor. Moreover, other studies have shown p110α to be the main isoform involved in mediating insulin signalling in 3T3-L1 cells [64,65]. These results correlated well with the effects seen on Topo IIα expression, which was strongly regulated by p110α. We also observed a reduction in the expression of Topo IIα following the inhibition of p110β and p110δ but high concentrations of the inhibitors were required, *i.e.* 10 μM. Therefore, p110α seems to be the major regulator of adipogenesis and expression of Topo IIα, while p110β and δ may have some more minor contributions since high concentrations of the inhibitors may not be reliable and lead to unspecific effects. However, the p110β inhibitor, TGX-221, has been reported to be selective and without off-target effects when used at 10 μM, although it is reported to cross-react with p110δ [66].

5. Conclusions

In summary, we have shown that Topo IIα expression peaks at the early stages of 3T3-L1 differentiation into adipocytes in a PI3K/mTOR-dependent manner and that it is essential for adipogenesis. All isoforms of the catalytic class IA PI3K seem to contribute, although p110α is the most dominant. The timing of Topo IIα expression coincides with the MCE phase where Topo IIα seems to have a role maybe in the replication of the heterochromatin regions, and perhaps in chromatin structure. Inhibiting Topo II after MCE and therefore when the expression of Topo IIα has declined has less effect on differentiation and expression of PPARγ, hence pointing to an important role in the early stages of differentiation for terminal differentiation. The results of this study may have implications in cancer considering that Topo II enzymes are targets of chemotherapy agents [67]. Thus, inhibition of Topo II in the course of cancer chemotherapy may have deleterious effects on the integrity of the adipose tissue which may have implications in the treatment of cancer in diabetic patients. Indeed, the chemotherapeutic Doxorubicin, which inhibits Topo II, has side effects with great loss of adipose tissue and muscle mass, was shown in a recent study to induce hyperglycemia and insulin resistance in rat [68].

Conflict of interest

The authors declare no conflict of interest.

Acknowledgments

This project was supported by grants from Helse Bergen Vest (project number 911682), The Norwegian Diabetes Foundation and the Meltzer Foundation.

Appendix A. Supplementary data

Supplementary data to this article can be found online at http://dx.doi.org/10.1016/j.cellsig.2016.07.002.

References

[1] E.J. Gallagher, D. LeRoith, Obesity and diabetes: the increased risk of cancer and cancer-related mortality, Physiol. Rev. 95 (3) (2015) 727–748.
[2] R. Berry, E. Jeffery, M.S. Rodeheffer, Weighing in on adipocyte precursors, Cell Metab. 19 (1) (2014) 8–20.
[3] H. Green, M. Meuth, An established pre-adipose cell line and its differentiation in culture, Cell 3 (2) (1974) 127–133.
[4] Q.Q. Tang, T.C. Otto, M.D. Lane, Mitotic clonal expansion: a synchronous process required for adipogenesis, Proc. Natl. Acad. Sci. U. S. A. 100 (1) (2003) 44–49.
[5] M. Reichert, D. Eick, Analysis of cell cycle arrest in adipocyte differentiation, Oncogene 18 (2) (1999) 459–466.
[6] Q.Q. Tang, M.D. Lane, Adipogenesis: from stem cell to adipocyte, Annu. Rev. Biochem. 81 (2012) 715–736.

[7] L. Guo, X. Li, Q.Q. Tang, Transcriptional regulation of adipocyte differentiation: a central role for CCAAT/enhancer-binding protein (C/EBP) beta, J. Biol. Chem. 290 (2) (2015) 755–761.
[8] L. Fajas, Re-thinking cell cycle regulators: the cross-talk with metabolism, Front. Oncol. 3 (2013) 4.
[9] Y.M. Patel, M.D. Lane, Mitotic clonal expansion during preadipocyte differentiation: calpain-mediated turnover of p27, J. Biol. Chem. 275 (23) (2000) 17653–17660.
[10] A. Abella, P. Dubus, M. Malumbres, S.G. Rane, H. Kiyokawa, A. Sicard, F. Vignon, D. Langin, M. Barbacid, L. Fajas, Cdk4 promotes adipogenesis through PPARgamma activation, Cell Metab. 2 (4) (2005) 239–249.
[11] D.A. Sarruf, I. Iankova, A. Abella, S. Assou, S. Miard, L. Fajas, Cyclin D3 promotes adipogenesis through activation of peroxisome proliferator-activated receptor gamma, Mol. Cell. Biol. 25 (22) (2005) 9985–9995.
[12] P. Hallenborg, R.K. Petersen, S. Feddersen, U. Sundekilde, J.B. Hansen, B. Blagoev, L. Madsen, K. Kristiansen, PPARgamma ligand production is tightly linked to clonal expansion during initiation of adipocyte differentiation, J. Lipid Res. 55 (12) (2014) 2491–2500.
[13] L.C. Foukas, D.J. Withers, Phosphoinositide signalling pathways in metabolic regulation, Curr. Top. Microbiol. Immunol. 346 (2010) 115–141.
[14] M.P. Czech, M. Tencerova, D.J. Pedersen, M. Aouadi, Insulin signalling mechanisms for triacylglycerol storage, Diabetologia 56 (5) (2013) 949–964.
[15] J. Boucher, A. Kleinridders, C.R. Kahn, Insulin receptor signaling in normal and insulin-resistant states, Cold Spring Harb. Perspect. Biol. 6 (1) (2014).
[16] A. Gagnon, C.S. Chen, A. Sorisky, Activation of protein kinase B and induction of adipogenesis by insulin in 3T3-L1 preadipocytes: contribution of phosphoinositide-3,4,5-trisphosphate versus phosphoinositide-3,4-bisphosphate, Diabetes 48 (4) (1999) 691–698.
[17] T.D. Bunney, M. Katan, Phosphoinositide signalling in cancer: beyond PI3K and PTEN, Nat. Rev. Cancer 10 (5) (2010) 342–352.
[18] R.S. Salamon, J.M. Backer, Phosphatidylinositol-3,4,5-trisphosphate: tool of choice for class I PI 3-kinases, BioEssays 35 (7) (2013) 602–611.
[19] G. Tzivion, M. Dobson, G. Ramakrishnan, FoxO transcription factors; regulation by AKT and 14-3-3 proteins, Biochim. Biophys. Acta 1813 (11) (2011) 1938–1945.
[20] X.D. Peng, P.Z. Xu, M.L. Chen, A. Hahn-Windgassen, J. Skeen, J. Jacobs, D. Sundararajan, W.S. Chen, S.E. Crawford, K.G. Coleman, N. Hay, Dwarfism, impaired skin development, skeletal muscle atrophy, delayed bone development, and impeded adipogenesis in mice lacking Akt1 and Akt2, Genes Dev. 17 (11) (2003) 1352–1365.
[21] J. Xu, K. Liao, Protein kinase B/AKT 1 plays a pivotal role in insulin-like growth factor-1 receptor signaling induced 3T3-L1 adipocyte differentiation, J. Biol. Chem. 279 (34) (2004) 35914–35922.
[22] S.J. Yun, E.K. Kim, D.F. Tucker, C.D. Kim, M.J. Birnbaum, S.S. Bae, Isoform-specific regulation of adipocyte differentiation by Akt/protein kinase Balpha, Biochem. Biophys. Res. Commun. 371 (1) (2008) 138–143.
[23] J.E. Kim, P.R. Shepherd, C. Chaussade, Investigating the role of class-IA PI 3-kinase isoforms in adipocyte differentiation, Biochem. Biophys. Res. Commun. 379 (4) (2009) 830–834.
[24] T. Maiuri, J. Ho, V. Stambolic, Regulation of adipocyte differentiation by distinct subcellular pools of protein kinase B (PKB/Akt), J. Biol. Chem. 285 (20) (2010) 15038–15047.
[25] X. Xia, G. Serrero, Inhibition of adipose differentiation by phosphatidylinositol 3-kinase inhibitors, J. Cell. Physiol. 178 (1) (1999) 9–16.
[26] J. Nitiss, DNA topoisomerase II and its growing repertoire of biological functions, Nat. Rev. Cancer (2009).
[27] S. Vos, E. Tretter, B. Schmidt, J. Berger, All tangled up: how cells direct, manage and exploit topoisomerase function, Nat. Rev. Mol. Cell Biol. 12 (12) (2011) 827–841.
[28] J.C. Wang, Cellular roles of DNA topoisomerases: a molecular perspective, Nat. Rev. Mol. Cell Biol. 3 (6) (2002) 430–440.
[29] G. Capranico, S. Tinelli, C.A. Austin, M.L. Fisher, F. Zunino, Different patterns of gene expression of topoisomerase II isoforms in differentiated tissues during murine development, Biochim. Biophys. Acta 1132 (1) (1992) 43–48.
[30] V.K. Tiwari, L. Burger, V. Nikoletopoulou, R. Deogracias, S. Thakurela, C. Wirbelauer, J. Kaut, R. Terranova, L. Hoerner, C. Mielke, F. Boege, R. Murr, A.H. Peters, Y.A. Barde, D. Schubeler, Target genes of Topoisomerase IIbeta regulate neuronal survival and are defined by their chromatin state, Proc. Natl. Acad. Sci. U. S. A. 109 (16) (2012) E934–E943.
[31] K. Tsutsui, K. Tsutsui, S. Okada, M. Watanabe, T. Shohmori, S. Seki, Y. Inoue, Molecular cloning of partial cDNAs for rat DNA topoisomerase II isoforms and their differential expression in brain development, J. Biol. Chem. 268 (25) (1993) 19076–19083.
[32] M. Watanabe, K. Tsutsui, K. Tsutsui, Y. Inoue, Differential expressions of the topoisomerase II alpha and II beta mRNAs in developing rat brain, Neurosci. Res. 19 (1) (1994) 51–57.
[33] F.H. Drake, G.A. Hofmann, H.F. Bartus, M.R. Mattern, S.T. Crooke, C.K. Mirabelli, Biochemical and pharmacological properties of p170 and p180 forms of topoisomerase II, Biochemistry 28 (20) (1989) 8154–8160.
[34] P.C. Goswami, J.L. Roti Roti, C.R. Hunt, The cell cycle-coupled expression of topoisomerase IIalpha during S phase is regulated by mRNA stability and is disrupted by heat shock or ionizing radiation, Mol. Cell. Biol. 16 (4) (1996) 1500–1508.
[35] R.D. Woessner, M.R. Mattern, C.K. Mirabelli, R.K. Johnson, F.H. Drake, Proliferation- and cell cycle-dependent differences in expression of the 170 kilodalton and 180 kilodalton forms of topoisomerase II in NIH-3T3 cells, Cell Growth Differ. 2 (4) (1991) 209–214.
[36] T.S. Mikkelsen, Z. Xu, X. Zhang, L. Wang, J.M. Gimble, E.S. Lander, E.D. Rosen, Comparative epigenomic analysis of murine and human adipogenesis, Cell 143 (1) (2010) 156–169.
[37] A. Soukas, N.D. Socci, B.D. Saatkamp, S. Novelli, J.M. Friedman, Distinct transcriptional profiles of adipogenesis in vivo and in vitro, J. Biol. Chem. 276 (36) (2001) 34167–34174.
[38] C. Guetg, R. Santoro, Formation of nuclear heterochromatin: the nucleolar point of view, Epigenetics 7 (8) (2012) 811–814.
[39] I. Usui, T. Haruta, M. Iwata, A. Takano, T. Uno, J. Kawahara, E. Ueno, T. Sasaoka, M. Kobayashi, Retinoblastoma protein phosphorylation via PI 3-kinase and mTOR pathway regulates adipocyte differentiation, Biochem. Biophys. Res. Commun. 275 (1) (2000) 115–120.
[40] W.C. Yeh, B.E. Bierer, S.L. McKnight, Rapamycin inhibits clonal expansion and adipogenic differentiation of 3T3-L1 cells, Proc. Natl. Acad. Sci. U. S. A. 92 (24) (1995) 11086–11090.
[41] S. Erener, M. Hesse, R. Kostadinova, M.O. Hottiger, Poly(ADP-ribose)polymerase-1 (PARP1) controls adipogenic gene expression and adipocyte function, Mol. Endocrinol. 26 (1) (2012) 79–86.
[42] M. Lehmann, E. Pirinen, A. Mirsaidi, F.A. Kunze, P.J. Richards, J. Auwerx, M.O. Hottiger, ARTD1-induced poly-ADP-ribose formation enhances PPARγ ligand binding and co-factor exchange, Nucleic Acids Res. 43 (1) (2015) 129–142.
[43] M. Sehested, P.B. Jensen, Mapping of DNA topoisomerase II poisons (etoposide, clerocidin) and catalytic inhibitors (aclarubicin, ICRF-187) to four distinct steps in the topoisomerase II catalytic cycle, Biochem. Pharmacol. 51 (7) (1996) 879–886.
[44] J. Roca, R. Ishida, J.M. Berger, T. Andoh, J.C. Wang, Antitumor bisdioxopiperazines inhibit yeast DNA topoisomerase II by trapping the enzyme in the form of a closed protein clamp, Proc. Natl. Acad. Sci. U. S. A. 91 (5) (1994) 1781–1785.
[45] S. Classen, S. Olland, J.M. Berger, Structure of the topoisomerase II ATPase region and its mechanism of inhibition by the chemotherapeutic agent ICRF-187, Proc. Natl. Acad. Sci. U. S. A. 100 (19) (2003) 10629–10634.
[46] Y.C. Cho, C.R. Jefcoate, PPARgamma1 synthesis and adipogenesis in C3H10T1/2 cells depends on S-phase progression, but does not require mitotic clonal expansion, J. Cell. Biochem. 91 (2) (2004) 336–353.
[47] M. Agostinho, J. Rino, J. Braga, F. Ferreira, S. Steffensen, J. Ferreira, Human topoisomerase IIalpha: targeting to subchromosomal sites of activity during interphase and mitosis, Mol. Biol. Cell 15 (5) (2004) 2388–2400.
[48] Q.Q. Tang, M.D. Lane, Activation and centromeric localization of CCAAT/enhancer-binding proteins during the mitotic clonal expansion of adipocyte differentiation, Genes Dev. 13 (17) (1999) 2231–2241.
[49] R.M. Umek, A.D. Friedman, S.L. McKnight, CCAAT-enhancer binding protein: a component of a differentiation switch, Science 251 (4991) (1991) 288–292.
[50] S.F. Li, L. Guo, S.W. Qian, Y. Liu, Y.Y. Zhang, Z.C. Zhang, Y. Zhao, J.Y. Shou, Q.Q. Tang, X. Li, G9a is transactivated by C/EBPbeta to facilitate mitotic clonal expansion during 3T3-L1 preadipocyte differentiation, Am. J. Physiol. Endocrinol. Metab. 304 (9) (2013) E990–E998.
[51] V. Gaggioli, B. Le Viet, T. Germe, O. Hyrien, DNA topoisomerase IIalpha controls replication origin cluster licensing and firing time in *Xenopus* egg extracts, Nucleic Acids Res. 41 (15) (2013) 7313–7331.
[52] T. Germe, O. Hyrien, Topoisomerase II-DNA complexes trapped by ICRF-193 perturb chromatin structure, EMBO Rep. 6 (8) (2005) 729–735.
[53] R. Gomez, P.W. Jordan, A. Viera, M. Alsheimer, T. Fukuda, R. Jessberger, E. Llano, A.M. Pendas, M.A. Handel, J.A. Suja, Dynamic localization of SMC5/6 complex proteins during mammalian meiosis and mitosis suggests functions in distinct chromosome processes, J. Cell Sci. 126 (Pt 18) (2013) 4239–4252.
[54] M.M. Dawlaty, L. Malureanu, K.B. Jeganathan, E. Kao, C. Sustmann, S. Tahk, K. Shuai, R. Grosschedl, J.M. van Deursen, Resolution of sister centromeres requires RanBP2-mediated SUMOylation of topoisomerase IIalpha, Cell 133 (1) (2008) 103–115.
[55] G.J. Gorbsky, Cell cycle progression and chromosome segregation in mammalian cells cultured in the presence of the topoisomerase II inhibitors ICRF-187 [(+)-1,2-bis(3,5-dioxopiperazinyl-1-yl)propane; ADR-529] and ICRF-159 (Razoxane), Cancer Res. 54 (4) (1994) 1042–1048.
[56] S. Isik, K. Sano, K. Tsutsui, M. Seki, T. Enomoto, H. Saitoh, K. Tsutsui, The SUMO pathway is required for selective degradation of DNA topoisomerase IIbeta induced by a catalytic inhibitor ICRF-193(1), FEBS Lett. 546 (2–3) (2003) 374–378.
[57] H. Xiao, Y. Mao, S.D. Desai, N. Zhou, C.Y. Ting, J. Hwang, L.F. Liu, The topoisomerase IIbeta circular clamp arrests transcription and signals a 26S proteasome pathway, Proc. Natl. Acad. Sci. U. S. A. 100 (6) (2003) 3239–3244.
[58] M.B. Hossain, P. Ji, R. Anish, R.H. Jacobson, S. Takada, Poly(ADP-ribose) polymerase 1 interacts with nuclear respiratory factor 1 (NRF-1) and plays a role in NRF-1 transcriptional regulation, J. Biol. Chem. 284 (13) (2009) 8621–8632.
[59] B.G. Ju, V.V. Lunyak, V. Perissi, I. Garcia-Bassets, D.W. Rose, C.K. Glass, M.G. Rosenfeld, A topoisomerase IIbeta-mediated dsDNA break required for regulated transcription, Science 312 (5781) (2006) 1798–1802.
[60] K.W. Trotter, H.A. King, T.K. Archer, Glucocorticoid receptor transcriptional activation via the BRG1-dependent recruitment of TOP2beta and Ku70/86, Mol. Cell. Biol. 35 (16) (2015) 2799–2817.
[61] R.H. Wong, I. Chang, C.S. Hudak, S. Hyun, H.Y. Kwan, H.S. Sul, A role of DNA-PK for the metabolic gene regulation in response to insulin, Cell 136 (6) (2009) 1056–1072.
[62] K. Tomiyama, H. Nakata, H. Sasa, S. Arimura, E. Nishio, Y. Watanabe, Wortmannin, a specific phosphatidylinositol 3-kinase inhibitor, inhibits adipocytic differentiation of 3T3-L1 cells, Biochem. Biophys. Res. Commun. 212 (1) (1995) 263–269.
[63] T. Asano, A. Kanda, H. Katagiri, M. Nawano, T. Ogihara, K. Inukai, M. Anai, Y. Fukushima, Y. Yazaki, M. Kikuchi, R. Hooshmand-Rad, C.H. Heldin, Y. Oka, M. Funaki, p110beta is up-regulated during differentiation of 3T3-L1 cells and contributes to the highly insulin-responsive glucose transport activity, J. Biol. Chem. 275 (23) (2000) 17671–17676.
[64] Z.A. Knight, B. Gonzalez, M.E. Feldman, E.R. Zunder, D.D. Goldenberg, O. Williams, R. Loewith, D. Stokoe, A. Balla, B. Toth, T. Balla, W.A. Weiss, R.L. Williams, K.M. Shokat,

A pharmacological map of the PI3-K family defines a role for p110alpha in insulin signaling, Cell 125 (4) (2006) 733–747.
[65] C. Chaussade, G.W. Rewcastle, J.D. Kendall, W.A. Denny, K. Cho, L.M. Grønning, M.L. Chong, S.H. Anagnostou, S.P. Jackson, N. Daniele, P.R. Shepherd, Evidence for functional redundancy of class IA PI3K isoforms in insulin signalling, Biochem. J. 404 (3) (2007) 449–458.
[66] S. Jamieson, J.U. Flanagan, S. Kolekar, C. Buchanan, J.D. Kendall, W.J. Lee, G.W. Rewcastle, W.A. Denny, R. Singh, J. Dickson, B.C. Baguley, P.R. Shepherd, A drug targeting only p110alpha can block phosphoinositide 3-kinase signalling and tumour growth in certain cell types, Biochem. J. 438 (1) (2011) 53–62.
[67] J.E. Deweese, N. Osheroff, The DNA cleavage reaction of topoisomerase II: wolf in sheep's clothing, Nucleic Acids Res. 37 (3) (2009) 738–748.
[68] E.A. de Lima Junior, A.S. Yamashita, G.D. Pimentel, L.G.O. De Sousa, R.V.T. Santos, C.L. Gonçalves, E.L. Streck, F.S. de Lira, J.C. Rosa Neto, Doxorubicin caused severe hyperglycaemia and insulin resistance, mediated by inhibition in AMPk signalling in skeletal muscle, J. Cachex. Sarcopenia Muscle (2016) (n/a-n/a).